BIOCHEMISTRY
including biophysical chemistry & molecular biology

Article

pubs.acs.org/biochemistry

Human SAS-6 C-Terminus Nucleates and Promotes Microtubule Assembly *in Vitro* by Binding to Microtubules

Hindol Gupta, Binshad Badarudeen, Athira George, Geethu Emily Thomas, K. K. Gireesh, and Tapas K. Manna*

School of Biology, Indian Institute of Science Education and Research Thiruvananthapuram, CET Campus, Thiruvananthapuram 695016, Kerala, India

Supporting Information

ABSTRACT: Centrioles are essential components of the animal centrosome and play crucial roles in the formation of cilia and flagella. They are cylindrical structures composed of nine triplet microtubules organized around a central cartwheel. Recent studies have identified spindle assembly abnormal protein SAS-6 as a critical component necessary for formation of the cartwheel. However, the molecular details of how the cartwheel participates in centriolar microtubule assembly have not been clearly understood. In this report, we show that the C-terminal tail (residues 470−657) of human SAS-6, HsSAS-6 C, the region that has been shown to extend toward the centriolar wall where the microtubule triplets are organized, nucleated and induced microtubule polymerization *in vitro*. The N-terminus (residues 1−166) of HsSAS-6, the domain known to be involved in formation of the central hub of the cartwheel, did not, however, exert any effect on microtubule polymerization. HsSAS-6 C bound to the microtubules and localized along the lengths of the microtubules *in vitro*. Microtubule pull-down and coimmunoprecipitation (Co-IP) experiments with S-phase synchronized HeLa cell lysates showed that the endogenous HsSAS-6 coprecipitated with the microtubules, and it mediated interaction with tubulin. Isothermal calorimetry titration and size exclusion chromatography showed that HsSAS-6 C bound to the $\alpha\beta$-tubulin dimer *in vitro*. The results demonstrate that HsSAS-6 possesses an intrinsic microtubule assembly promoting activity and further implicate that its outer exposed C-terminal tail may play critical roles in microtubule assembly and stabilizing microtubule attachment with the centriolar cartwheel.

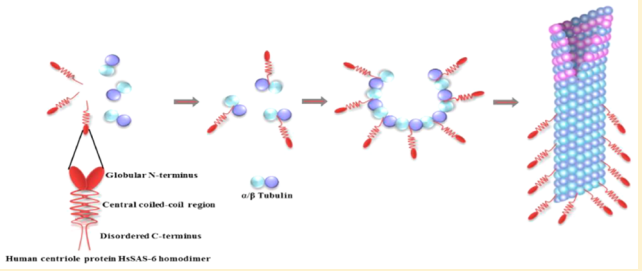

Centrosome acts as the main microtubule organizing center (MTOC) of most animal cells and regulates processes such as cell division, cell polarization, and biogenesis of cilia. It consists of a pair of centrioles surrounded by a cloud of pericentriolar material (PCM) proteins.[1,2] The two centrioles of a centrosome are duplicated once in every cell cycle during the S phase, giving rise to two pairs of centrioles, which eventually mature into two centrosomes. The duplicated centrosomes form the spindle-organizing centers (poles) during mitosis and are inherited equally by the daughter cells.[3,4] In addition to mitosis-specific roles, centrioles are essential for the assembly of primary and motile cilia. The mother centriole of centrosome after its maturation forms the basal body, the main protein-rich platform onto which the cilia are assembled.[5−7] Defects in centriolar microtubule assembly have been linked to cell division defects and cilia dysfunctions.[5]

Centriole duplication involves formation and maturation of the daughter centriole from the proximal side of each of the existing centrioles, the mother centrioles, followed by disengagement of the mother centrioles. Each centriole assembles nine sets of triplet microtubules organized along its wall.[5,6] During the initial step of centriole assembly, a protein-rich cartwheel structure consisting of a central hub connected with nine spokes projecting outward is formed.[8,9] As the cartwheel grows, the triplet microtubules are assembled at the proximal end of each spoke. This minimal structure is referred to as the pro-centriole. Each mother centriole is restricted to form only one procentriole from its proximal end, which eventually grows into a matured centriole with an elongated barrel and the triplet microtubules. Although the cartwheel-like ring complex is essential for organizing the triplet microtubules in the centriole, the mechanism underlying the ring complex-microtubule interaction remains poorly understood. Spindle assembly abnormal protein 6 (SAS-6) has recently been shown to be a key protein necessary for formation of the centriolar cartwheel.[10,11] SAS-6 is a coiled-coil protein highly conserved in most eukaryotes and is recruited to centrioles at the onset of centrosome duplication cycle.[3] SAS-6 consists of an N-terminal globular domain which forms the central hub of the cartwheel, followed by a central coiled-coil domain, which forms spokes of the wheel and a relatively less characterized C-terminal tail region.[10,11]

Evidence from high-resolution electron microscopy analyses of the human centriole has shown the presence of three types of microtubules, A, B, and C, in the centriole.[12] Formation of

Received: September 4, 2015
Published: September 30, 2015

DOI: 10.1021/acs.biochem.5b00978
Biochemistry 2015, 54, 6413−6422

the triplet is initiated with nucleation of A-microtubules presumably by recruiting γ-tubulin ring complex proteins on the pro-centriole cartwheel.[12] The A microtubule then acts as the template for assembly of the B microtubule, and subsequently, the B microtubule acts as the template for C-microtubule assembly.[12] While the proteins like CPAP, and CEP family protein, CEP135 are potential factors known to be involved in the assembly of the A microtubules,[13,14] factors and mechanisms involved in the assembly of B and C microtubules are not clearly known. Furthermore, though CEP135 has been shown to be critical for stabilization of the microtubule triplets, it does not seem to be indispensable for centriolar microtubule assembly as its loss does not substantially affect the overall microtubule density in the centrioles.[13] For example, loss of Bld10p, the *chlamydomonas* ortholog of human CEP135 has been shown to result in centrioles with eight triplet microtubules instead of nine.[15,16] Similarly, in human cells, CEP135 depletion results in reduced numbers of microtubule triplets (five and seven).[13] These findings suggested that additional components are involved in the nucleation and assembly of centriolar microtubule triplets. Recent studies have shown that the cartwheel itself can associate with the microtubules independent of CEP135.[13] Additionally, depletion of SAS-6 has been shown to reduce the microtubule numbers substantially in both *Chlamydomonas* and *Drosophila* centrioles.[10,17] These findings suggest that SAS-6 itself has a direct role in the regulation of centriolar microtubule formation.

In this work, we have investigated the role of human SAS-6 in regulation of microtubules *in vitro*. Because the C-terminal tail of SAS-6 projects outward toward the wall of the centriole where the triplets microtubules are organized,[10,13,18] and it has been shown to be involved in proper organization of centriolar components and centriole duplication *in vivo*,[19] we hypothesized that the C-terminus could play an important role in microtubule assembly and cartwheel−microtubule interaction. We found that human SAS-6 C terminus (470−657) (HsSAS-6 C), but not its N-terminus, induced nucleation of microtubule polymerization and promoted microtubule assembly *in vitro*. Sedimentation assay and immunofluorescence imaging showed that HsSAS-6 C bound to the microtubules along their lengths *in vitro*. Biochemical experiments with cell lysates showed that the endogenous HsSAS-6 interacts with tubulin and microtubules. Isothermal titration calorimetry and gel filtration analyses with purified proteins further showed that HsSAS-6 C bound to tubulin dimers. The results demonstrate that HsSAS-6 C-terminus possesses an intrinsic microtubule assembly promoting activity and further implicate a direct role of HsSAS-6 in centriolar microtubule assembly in addition to the proteins known to regulate this process.

MATERIALS AND METHODS

Materials. GTP, PIPES, thymidine, taxol, and EGTA were obtained from Sigma (St. Louis, U.S.A.). Mouse monoclonal anti-HsSAS-6 (1−300) and mouse monoclonal anti-HsSAS-6 (404−657) were obtained from Santa Cruz Biotechnology, Inc. (U.S.A.). Mouse monoclonal α-tubulin antibody was obtained from Sigma (St. Louis, U.S.A.), rabbit anti-α-tubulin was obtained from Cell Signaling (Denver, U.S.A.), and rat monoclonal anti-α-tubulin was purchased from Novus Biologicals (San Dieogo, U.S.A.) The secondary antimouse FITC-conjugated antibody was purchased from Jackson Immuno Research (U.S.A.). Rhodamine-labeled tubulin was obtained from Cytoskeleton (U.S.A.).

Plasmids and Proteins. The plasmids encoding HsSAS-6 N (1−166), HsSAS-6 C (470−657), and HsSAS-6 C′ (546−638) of HsSAS-6 were generated from the cDNA of full-length HsSAS-6 (kindly provided by Pierre Gönzcy, Swiss Institute for Experimental Cancer Research, SW) by PCR and subcloned into the pET28a vector (Novagen), containing an N-terminal 6x-His tag. The resulting plasmids were transformed into BL21 (DE3) cells for protein expression. As HsSAS-6 N and HsSAS-6 C exhibited poor solubility, urea-induced denaturation-renaturation method was followed to obtain the pure proteins.[20] Briefly, cells expressing 6x-His-tagged HsSAS-6 N or HsSAS-6 C were grown under induction of IPTG (1 mM) at 37 °C for 4 h, centrifuged at 7000 rpm for 10 min. The cell pellets were lysed with lysis buffer (30 mM Tris, 500 mM NaCl, 0.1 mM DTT, 1 mM PMSF, pH 7.4) and then centrifuged at 16 000 rpm for 90 min. The pellets were washed with wash buffer (30 mM Tris, 500 mM NaCl, 0.5% Triton X-100, pH-7.4) and were resuspended in 10 mM $CaCl_2$ followed by centrifugation at 16 000 rpm. The pellets obtained after centrifugation were dissolved in the extraction buffer containing 8 M urea, 30 mM Tris, 500 mM NaCl, pH 7.4 and then centrifuged at 16 000 rpm for 90 min at room temperature.[19] The supernatants were loaded into an Ni^{2+}-NTA column, and washed with wash buffer (8 M urea, 30 mM Tris, 500 mM NaCl, 20 mM imidazole, pH 7.4). Pure proteins were obtained by elution using buffer containing 8 M urea, 30 mM Tris, 100 mM NaCl, 400 mM imidazole, pH 7.4. The purity of eluted proteins was verified by SDS-PAGE followed by Coomassie blue staining. Fractions containing HsSAS-6 N or HsSAS-6 C with high degree of purity were pooled and allowed to refold by stepwise removal of urea through dialysis against the buffer, 30 mM Tris, 150 mM NaCl, 3 mM DTT, pH-7.4. HsSAS-6 C′ was soluble in the lysis buffer and was purified directly by Ni^{2+}-NTA column without using urea. Proteins were estimated using the Bradford method with BSA as standard.[21]

Isolation of Tubulin. Tubulin was purified from goat brains by the cycles of temperature-dependent assembly and disassembly as previously described.[22]

Microtubule Polymerization Assay. Tubulin (10 μM) was polymerized with different concentrations of HsSAS-6 C or HsSAS-6 N in PEM (50 mM PIPES, 1 mM EGTA, 0.5 mM $MgCl_2$) buffer supplemented with 1 mM GTP at pH 7.0. The kinetics of tubulin polymerization was assessed at 37 °C for 30 min by measuring the turbidity at 360 nm using a Varian Cary 50 BIO UV VIS spectrophotometer.[23] The polymerized microtubules were pelleted after passing through a 15% sucrose cushion followed by centrifugation at 45 000 rpm for 45 min at 37 °C. The proteins in the pellets were analyzed by SDS-PAGE followed by Coomassie blue staining.

In Vitro Microtubule Imaging. A mixture of rhodamine-labeled and unlabeled tubulin (1 μM + 12 μM) was incubated with HsSAS-6 C (5 μM) at 37 °C for 15 min in PEM buffer supplemented with 1 mM GTP. The polymerized microtubules were fixed with 0.1% glutaraldehyde and diluted 1000 times in warm PEM buffer. The diluted microtubules were sedimented onto 0.1% poly-L-lysine coated glass coverslips and incubated with mouse monoclonal HsSAS-6 C antibody for 30 min followed by incubation with FITC-conjugated antimouse secondary antibody for 20 min.The images were captured by Leica SP5 laser confocal microscope. Intensity measurements were performed using the system run software provided by Leica. Briefly, the levels of HsSAS-6 C bound to the microtubules were quantified by measuring the intensity per

DOI: 10.1021/acs.biochem.5b00978
Biochemistry 2015, 54, 6413−6422

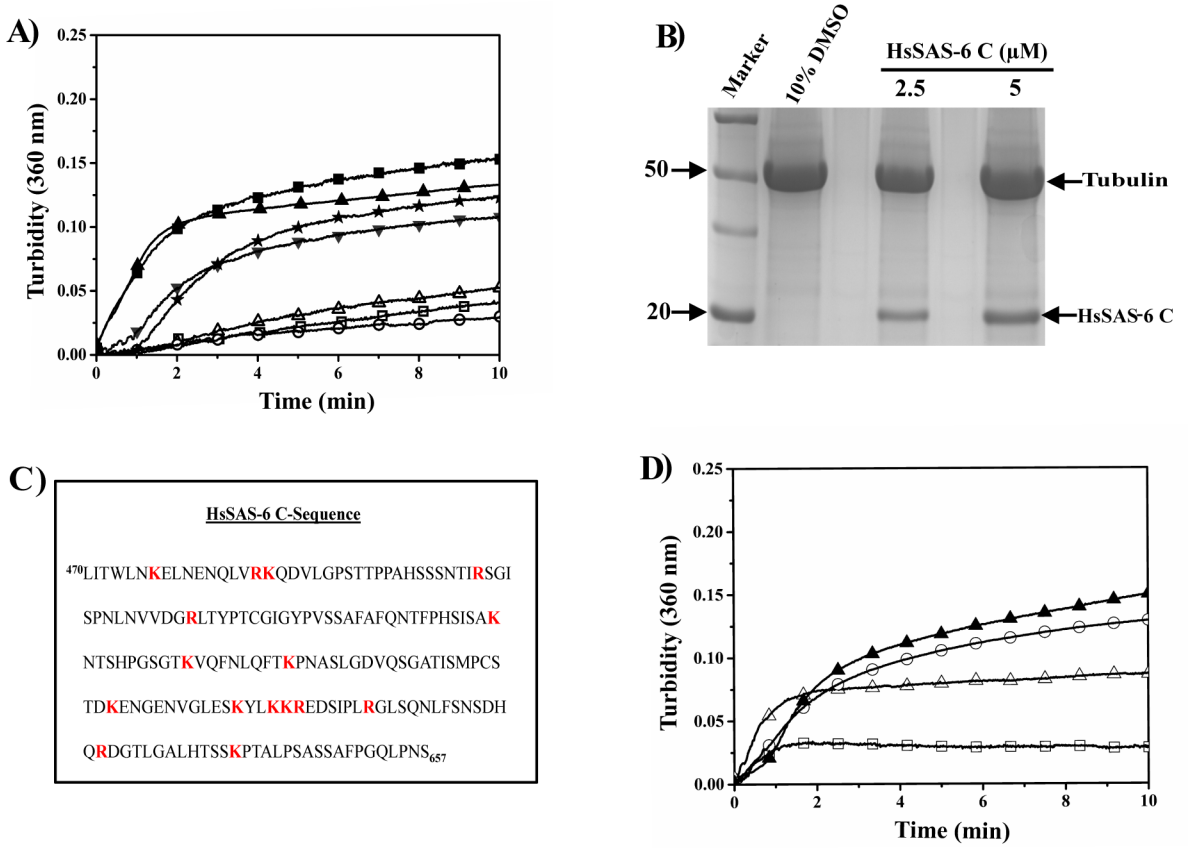

Figure 1. HsSAS-6 C nucleates and promotes microtubule polymerization *in vitro*. (A) Tubulin (10 μM) was polymerized in the absence (○) or presence of 2.5 (▼), 5 (▲), and 7.5 μM (■) HsSAS-6 C or HsSAS-6 N (7.5 μM) (Δ), and the polymerization was monitored by measuring turbidity at 360 nm. Polymerization of tubulin by DMSO (10%) as an inducer (★) is also shown. Negative control for HsSAS-6 C (without tubulin) 7.5 μM (□) is also shown. (B) Coomassie blue-stained SDS-PAGE (12% gel) loaded with proteins present in the microtubules polymerized either in the presence of HsSAS-6 C (2.5 and 5 μM) or DMSO (control). The microtubules were pelleted through 15% sucrose cushion prior to loading onto the gel. (C) Amino acid sequence of HsSAS-6 C (470−657) showing the positively charged lysines and arginines (shown by red). (D) Turbidity assay for tubulin polymerization induced by HsSAS-6 C (7.5 μM) in the absence (▲) or presence of 50 (○), 150 (Δ), and 250 mM (□) NaCl.

pixel of the selected regions (~24 numbers) of interest (ROI) of fixed area (1.9 μm^2) on individual microtubules in green channel (FITC stained HsSAS-6 C) normalized to the same in red channel (rhodamine-tubulin).

Microtubule Pull-Down from Cell Lysates. Hela cells grown in DMEM medium supplemented with 10% fetal bovine serum were synchronized in the S phase by incubating with 2 mM thymidine for 16 h and then lysed with lysis buffer containing 0.1 M PIPES, pH 6.6, 1 mM EGTA, 1 mM $MgSO_4$, 0.5% Triton X, 1 mM PMSF, protease inhibitor cocktail (Sigma), and phosphatase inhibitor cocktail (Sigma) and centrifuged at 55 000 rpm at 4 °C to separate the lysate from cell debris. The cell lysate was incubated with 20 μM taxol and 1 mM GTP at 37 °C for 30 min to polymerize microtubules and then centrifuged at 50 000 rpm for 1 h at 37 °C to pellet the microtubules. The pellet was washed three times with warm buffer and then dissolved in the SDS-PAGE sample buffer. The proteins were resolved by SDS−PAGE followed by Western blot using mouse monoclonal SAS 6 and mouse monoclonal α-tubulin antibodies.

Coimmunoprecipitation (Co-IP). HeLa cells grown in DMEM medium supplemented with 10% fetal bovine serum were synchronized at the S phase by treating the cells with 2 mM thymidine for 16 h before harvesting. The cells were lysed with lysis buffer (20 mM Tris pH 7.5, 50 mM NaCl, 1 mM EGTA, 1% Triton X-100, protease inhibitor, phosphatase inhibitor cocktail 2 and phosphate inhibitor 3), and the cell lysate was incubated with either mouse monoclonal SAS 6 antibody or rabbit α-tubulin antibody overnight at 4 °C, followed by incubation with protein G beads (Santa Cruz biotechnology, U.S.A.) for 2 h at 4 °C. The beads were washed with lysis buffer and then subjected to SDS−PAGE followed by immunoblot analysis. For immunoblotting of SAS-6 IP sample, mouse monoclonal SAS-6 and mouse monoclonal α-tubulin antibodies were used. For immunoblotting of α-tubulin IP sample, rat α-tubulin was used to probe tubulin in order to avoid interference with rabbit IgG band. Mouse monoclonal SAS-6 antibody was used to probe SAS-6 in the α-tubulin IP. The membranes were developed using the Immobilon reagent (Millipore, U.S.A.) and imaged using Chemi Doc XRS System (Bio-Rad, U.S.A.).

Determination of Dissociation Constant of HsSAS-6 C-Microtubule Binding in Vitro. Tubulin (20 μM) was polymerized in PEM buffer containing 1 mM GTP and 20 μM taxol at 37 °C for 15 min. The polymerized microtubules (10 μM) were incubated with different concentrations of HsSAS-6 C (1, 2, 3, 4, 6, and 8 μM) for 10 min at room temperature and then sedimented after passing through a 15% sucrose cushion followed by centrifugation at 45 000 rpm for 45 min at 37 °C. The separated pellet fractions were dissolved and loaded onto SDS-PAGE (12%). The intensities of Coomassie-stained bands of HsSAS-6 C in SDS-PAGE were measured by Quantity One

DOI: 10.1021/acs.biochem.5b00978
Biochemistry 2015, 54, 6413−6422

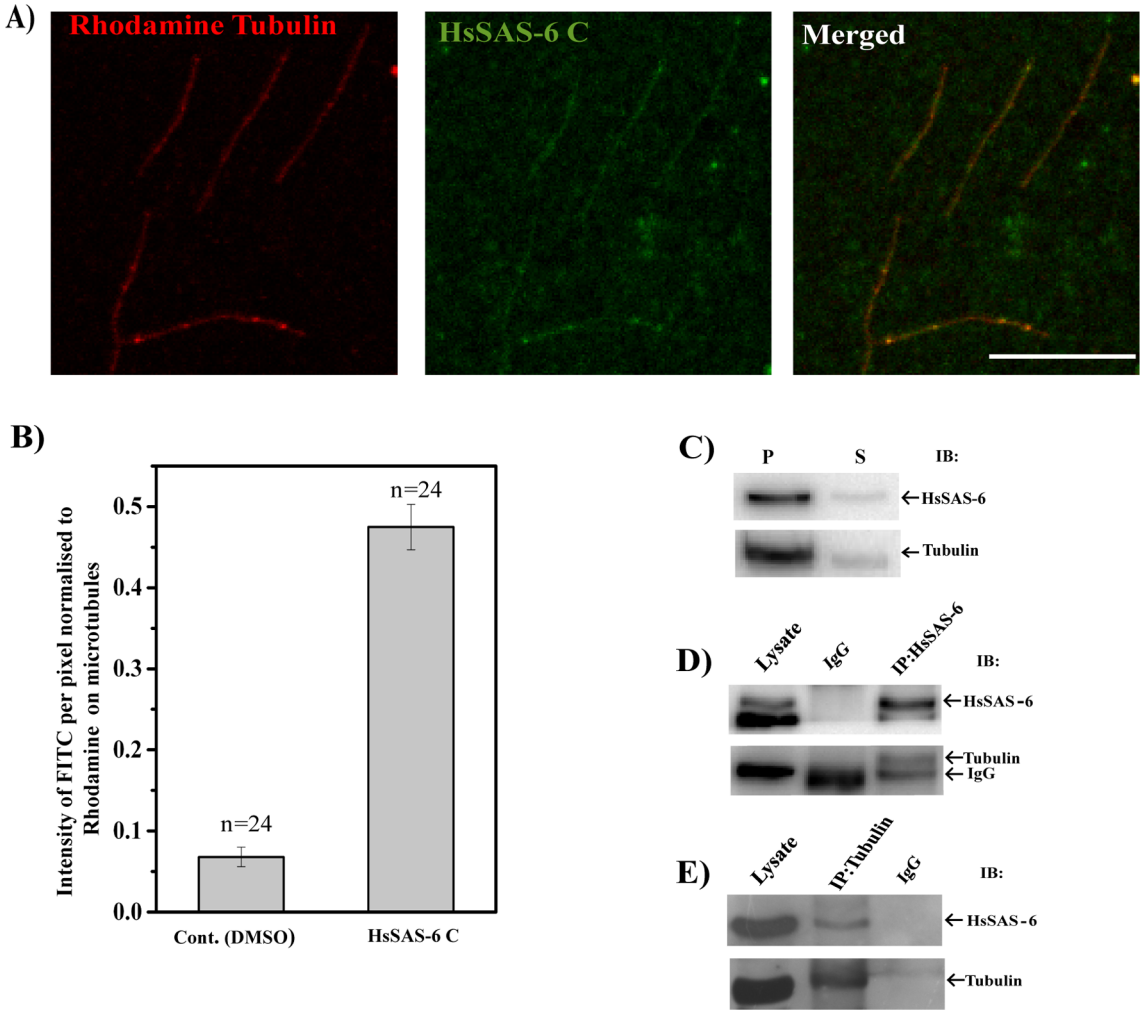

Figure 2. HsSAS-6 C localizes on the microtubules (A) Confocal micrographs of HsSAS-6 C-polymerized microtubules. Rhodamine-labeled tubulin (red) (unlabeled tubulin plus labeled tubulin, total ~13 μM) was polymerized into microtubules by HsSAS-6 C (5 μM), stained with mouse monoclonal HsSAS-6 C primary antibody followed by addition of secondary antibody conjugated with FITC (green) and imaged. The polymerized microtubules were diluted 1000 times prior to sediment onto the glass coverslips. Scale bar, 10 μm. (B) The plot depicts the quantification of HsSAS-6 C (FITC) intensity per pixel on the microtubule normalized to tubulin (rhodamine) intensity. Number of regions analyzed = 24. The intensity data were compared with the control DMSO-polymerized microtubules incubated with the FITC conjugated secondary antibody in the absence of HsSAS-6 C. The image of the DMSO-polymerized control microtubules are shown in Figure S2A of the Supporting Information. (C) Thymidine-treated S phase-synchronized HeLa cells were lysed, subjected to microtubule pull down assay, and analyzed by Western blot to assess the amount of HsSAS-6 associated with microtubule pellet (P). The proteins present in the unpolymerized fraction (S) were also probed. (D, E) HeLa cells were synchronized in the S-phase using thymidine block, lysed, and processed for coimmunoprecipitation (Co-IP) against HsSAS-6 or tubulin. (D) IP, immunoprecipitate of HsSAS-6; IB, immunoblot for HsSAS-6 and tubulin. (E) IP, immunoprecipitate of tubulin; IB, immunoblot for tubulin and HsSAS-6. Details on antibodies used in these experiments are provided in Materials and Methods.

software.[24] The background intensities of HsSAS-6 C were estimated by pelleting HsSAS-6 C through a sucrose cushion in the absence of microtubules. The corrected band intensities of HsSAS-6 C relative to the background were obtained by subtracting background intensities from the sample data. The dissociation constant (K_d) was determined by fitting the band intensities into the equation, $I_x = I_{max}\ C/(K_d + C)$,[24] using Origin 9.0 software, where I_x is the band intensity at any concentration of HsSAS-6 C, I_{max} is the maximum band intensity, and C is the concentration of HsSAS-6 C. The K_d is represented as mean ± SEM (two experiments). The effect of NaCl on the K_d of HsSAS-6 C-microtubule interaction was determined by incubating HasSAS-6 C with taxol-stabilized microtubules in the presence of 300 mM NaCl.

Size Exclusion Chromatography. The mixture of tubulin (15 μM) and HsSAS-6 C (10 μM) in PEM buffer (pH 7.0) preincubated at 4 °C for 15 min was loaded onto a Superdex-200 size exclusion column (Akta 10, GE Life Sciences, U.S.A.). The elution profile was obtained by measuring the absorbance at 280 nm. The eluted proteins were collected in fractions of 100 μL each, precipitated by ethanol, and analyzed by SDS-PAGE followed by Coomassie blue staining. Similar procedures were followed for tubulin (10 μM) and HsSAS-6 C (10 μM) control, respectively.

Isothermal Titration Calorimetry (ITC). HsSAS-6 N (10 μM) or HsSAS-6 C (10 μM) was titrated against tubulin (100 μM) at 25 °C using an ITC-200 Microcalorimeter of Microcal (Northampton, MA, USA). Each set of titrations involved 20 injections of tubulin (2 μL each) to HsSAS-6 N or HsSAS-6 C in the cell at 2 min interval with continuous stirring. The heat of dilution data corresponding to individual injections were analyzed using a binding model of one set of sites considering

DOI: 10.1021/acs.biochem.5b00978
Biochemistry 2015, 54, 6413−6422

one tubulin binding site per HsSAS-6 C molecule with system run Microcalorigin 7.0 software. The ΔH and ΔS values were obtained by fitting the data using nonlinear least-squares model. ΔG was calculated from Gibb's equation, $\Delta G = \Delta H - T\Delta S$.[25] The data are represented as the mean ± SEM from three sets of experiments.

RESULTS AND DISCUSSION

HsSAS-6 C Nucleates and Promotes Microtubule Assembly *in Vitro*. We first determined the effect of the C-terminal tail of human SAS-6 [HsSAS-6 C (470−657)] on microtubule polymerization *in vitro*. We also verified the effect of the N-terminus of human SAS-6 [HsSAS-6 N (1−166)], which has mostly been known to be involved in formation of the central hub of centriole cartwheel and is presumably not exposed to the centriolar microtubules. Both the domains were obtained with about 100% purity (Materials and Methods) (Figure S1A,B of the Supporting Information). The secondary structural contents of the purified proteins were also verified by circular dichroism (CD) spectroscopy. CD spectrum of HsSAS-6 C showed an absorption minimum at ∼205 nm with relatively low absorbance in the 220−225 nm region, suggesting that HsSAS-6 C is mostly unstructured (Figure S1C of the Supporting Information), as indicated in earlier studies.[11,13] CD spectrum of HsSAS-6 N showed two absorption minima, at ∼220 nm and ∼208 nm, respectively, (Figure S1D of the Supporting Information) implying that HsSAS-6 N possesses a distinct secondary structure as shown in previous studies.[26] Consistent with previous studies, our size exclusion chromatography analysis also showed that purified HsSAS-6 N exists in the dimer form[26] (data not shown).

The effect of HsSAS-6 C on microtubule assembly was determined *in vitro* by turbidity assay using purified tubulin (Figure 1A). HsSAS-6 C induced polymerization of tubulin dimer into microtubules in a dose-responsive manner in the absence of any polymerization inducer. HsSAS-6 C at a molar ratio of 0.5:1 to tubulin polymerized tubulin into microtubules to an extent similar to that observed with 10% DMSO as a polymerization inducer (Figure 1A). HsSAS-6 N, however, did not exhibit any microtubule-polymerizing activity under similar conditions (Figure 1A). To confirm that the increase of turbidity induced by HsSAS-6 C was due to formation of microtubule polymer and not due to mere aggregation of proteins present in the reaction mixture containing HsSAS-6 C and tubulin, the HsSAS-6 C-polymerized microtubules were verified for cold instability. HsSAS-6 C-polymerized microtubules depolymerized soon after incubation at 4 °C. The loss of turbidity was consistent with the contents of the solution containing microtubules (Figure S1E of the Supporting Information). The formation of microtubules by HsSAS6-C was also confirmed by transmission electron microscopy (data not shown). The effect of HsSAS-6 C on tubulin polymerization was also confirmed by microtubule cosedimentation assay followed by SDS-PAGE analysis (Figure 1B). Together, these results indicate that the C-terminal tail of HsSAS-6 possesses an intrinsic microtubule nucleating and assembly promoting activity. Microtubule associated proteins (MAPs) including MAP7D3 and kinesin are known to promote microtubule polymerization through binding of their regions rich with positively charged amino acids with the negatively charged C-terminal tails of the tubulin dimer.[24,27] The amino acid sequence of HsSAS-6 C showed that it is highly rich with positively charged amino acids including 10 lysines and 6 arginines (Figure 1C). It could be possible that the microtubule polymerizing activity of HsSAS-6 C is mediated through charge−charge interaction between its positively charged amino acids and the C-terminal tails of tubulin dimer. To test this hypothesis, we analyzed HsSAS-6 C-induced tubulin polymerization in the presence of NaCl, which can shield charge−charge interaction between proteins. Treatment of NaCl inhibited SAS-6 C-induced tubulin polymerization in a dose-dependent manner (Figure 1D).

HsSAS-6 C Binds to Microtubules and Localizes along Their Lengths *in Vitro*. As HsSAS-6 C was cosedimented with microtubules (Figure 1B), we then examined how it localized on the microtubules. This was performed by fluorescence-based imaging using rhodamine tubulin-labeled microtubules (Materials and Methods). The rhodamine tubulin-labeled microtubules polymerized by HsSAS-6 C were stained with HsSAS-6 C-specific antibody and imaged by confocal microscope. HsSAS-6 C localized along the lengths of the HsSAS-6 C-polymerized microtubules (Figure 2A). HsSAS-6 C-association with the microtubules was further confirmed by quantifying HsSAS-6 C intensity on the microtubules (Materials and Methods) (Figure 2B). To avoid any non-specific adherence of HsSAS-6 C antibody on the microtubules, the control DMSO-polymerized microtubules incubated with HsSAS-6 C-antibody in the absence of HsSAS-6 C were imaged. As expected, no HsSAS-6 C antibody staining on the control microtubules was observed (Figure S2B of Supporting Information). We also examined whether HsSAS-6 N could localize on the microtubules. As the N-terminus does not possess any microtubule polymerizing activity on its own (Figure 1A), its localization on the microtubules was inspected by using DMSO-polymerized microtubules. As expected, no association of HsSAS-6 N on the microtubules was observed (Figure S2B of the Supporting Information).

HsSAS-6 Interacts with Microtubules Polymerized *ex Vivo*. We next addressed whether the endogenous HsSAS-6 interacts with the microtubules polymerized from cell lysates. Cellular tubulin in thymidine-treated S phase-synchronized HeLa cell lysate was polymerized into microtubules by using 20 μM taxol, and the association of HsSAS-6 with the polymerized microtubules was assessed by cosedimentation analysis (Materials and Methods). HsSAS-6 was coprecipitated with the taxol-polymerized microtubules (Figure 2C). Consistent with a previous study in asynchronous HEK293T cells,[13] we also found that cosedimentation using asynchronous HeLa cell lysates did not show any detectable level of HsSAS-6 associated with the microtubules (data not shown). This suggests that HsSAS-6-microtubule interaction is cell cycle stage specific. HsSAS-6 is known to be ubiquitylated and degraded during the late S-phase and thereafter.[28] Therefore, the level of HsSAS-6 available to bind to the microtubules would be expected to be low in the asynchronous cell population. The minimum level that is still available can also undergo post-translational modification (e.g., ubiquitylation),[28,29] the process that may inhibit its association with the microtubules. We also performed coimmunoprecipitation (co-IP) to determine the interaction of HsSAS-6 with cellular tubulin in the thymidine-treated HeLa cell lysate. Tubulin was coprecipitated with HsSAS-6 (Figure 2D). This interaction was also confirmed with reverse IP in which HsSAS-6 was coprecipitated with tubulin (Figure 2E).

HsSAS-6 C Binds to the Microtubules with Considerably High Affinity *in vitro*. We next determined the binding affinity of HsSAS-6 C-microtubule interaction by

DOI: 10.1021/acs.biochem.5b00978
Biochemistry 2015, 54, 6413−6422

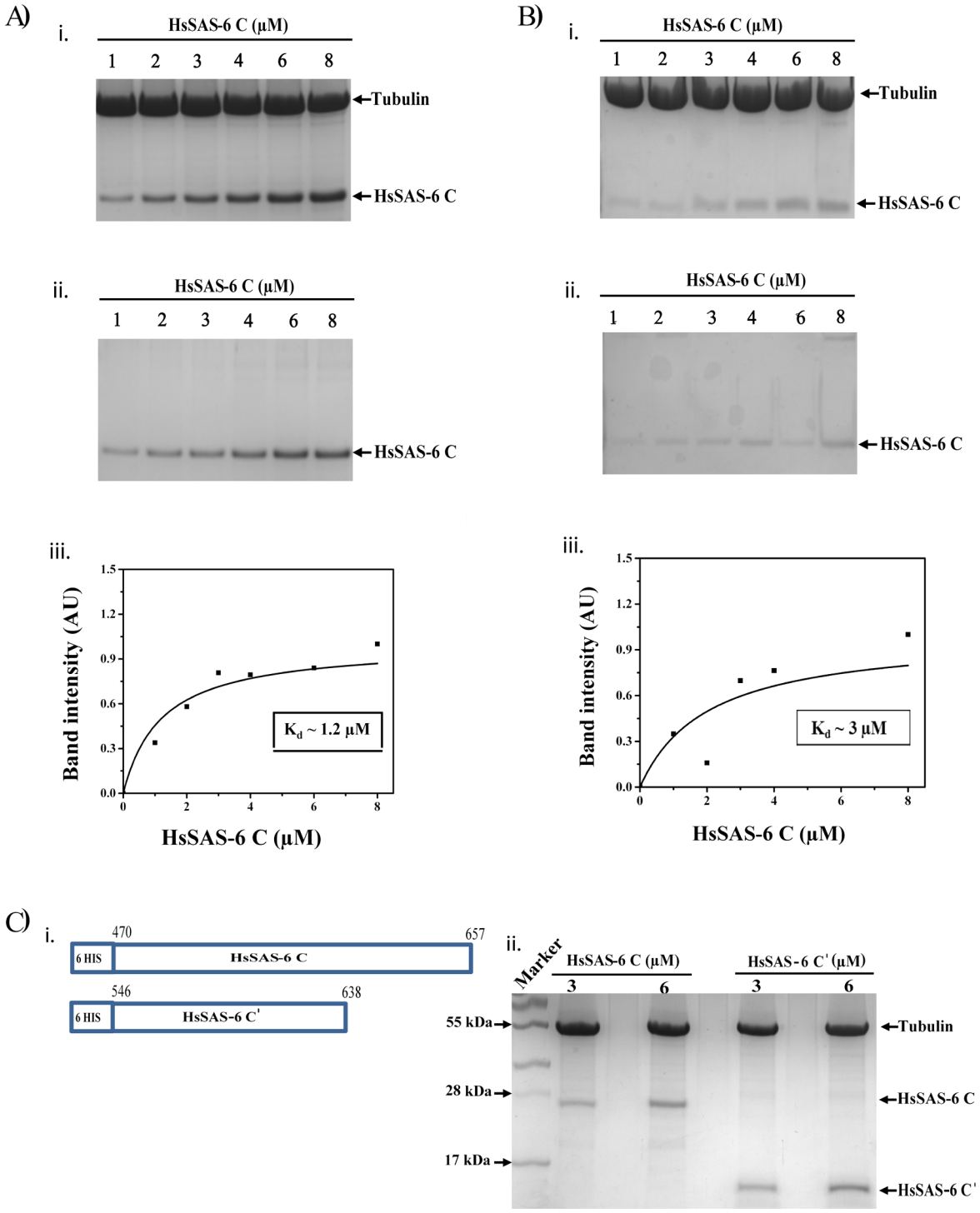

Figure 3. Binding of HsSAS-6 C with microtubules. Taxol-stabilized microtubules were incubated with different concentrations (1−8 μM) of HsSAS-6 C in the (A) absence or (B) presence of 300 mM NaCl. (i) of (A and B) Microtubule-bound HsSAS-6 C was estimated from the Coomassie blue stained SDS-PAGE (12%) gels loaded with sedimented microtubule and the bound HsSAS-6 C. (ii) of (A and B) Coomasie blue-stained SDS-PAGE loaded with control samples of HsSAS-6 C (1−8 μm) in the absence of microtubules after sedimentation. (iii) of (A and B) Plots of HsSAS-6 C concentrations vs corrected band intensities of HsSAS-6 C after background subtraction. K_d was determined by fitting the data points in a binding isotherm using Origin 7.0. (C) (i) Panels showing HsSAS-6 C and its truncated 546−638 region, HsSAS-6 C′. (ii) Coomassie blue-stained SDS-PAGE (12% gel) of proteins associated with the taxol-polymerized microtubules incubated with either HsSAS-6 C (3 and 6 μM) or HsSAS-6 C′ (3 and 6 μM).

cosedimenting HsSAS-6 C with taxol-polymerized steady-state microtubules *in vitro* followed by quantitation of HsSAS-6 C associated with the microtubule pellet (Materials and Methods). HsSAS-6 C bound to the microtubules with a considerably high affinity (K_d = 1 ± 0.2 μM) (Figure 3A). It is worth noting that microtubule binding affinity of HsSAS-6 C lies in the range similar to the binding affinities of several other microtubule associated proteins including MAP2 (K_d ≈ 1.1

DOI: 10.1021/acs.biochem.5b00978
Biochemistry 2015, 54, 6413−6422

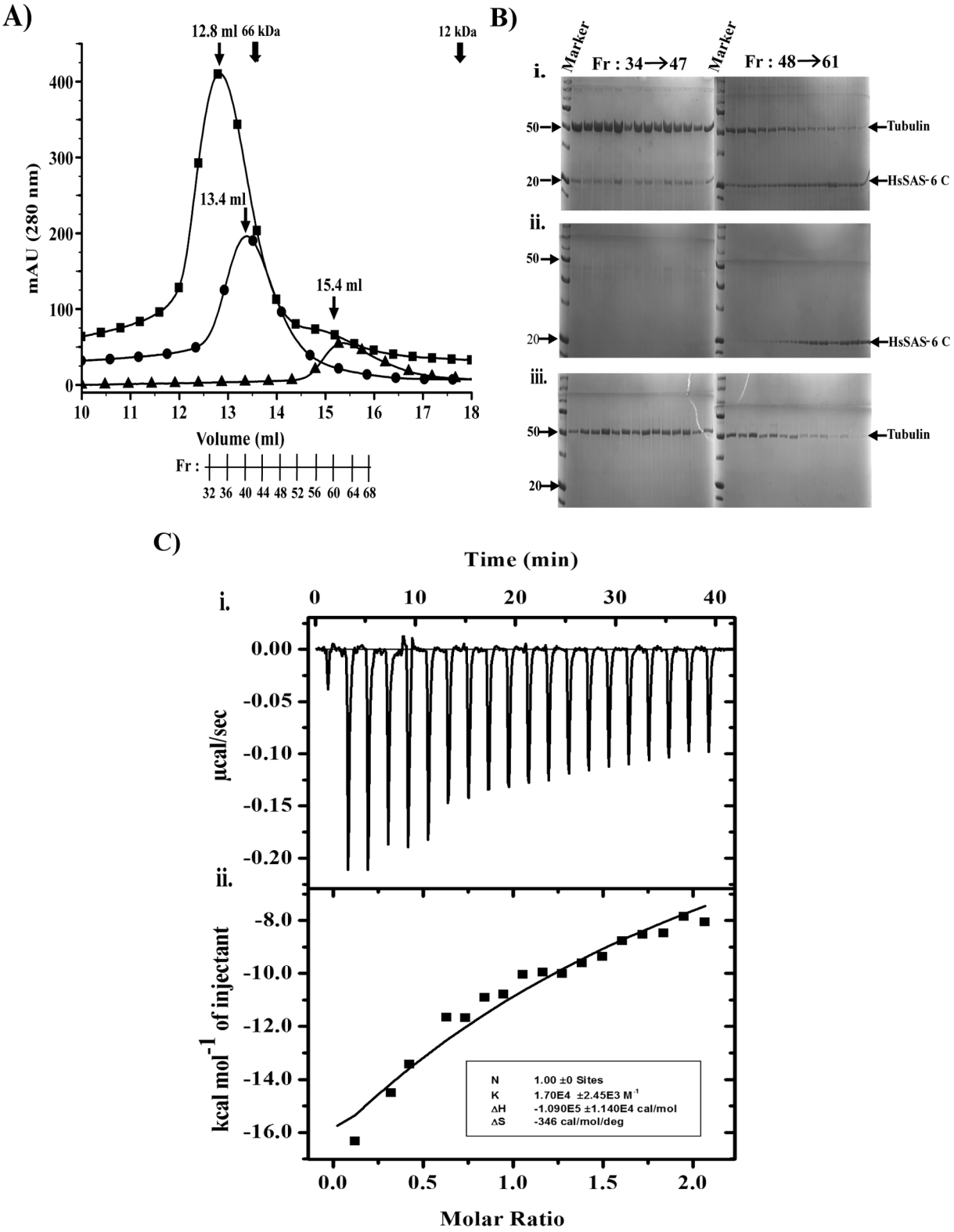

Figure 4. HsSAS-6 C binds to $\alpha\beta$-tubulin dimer. (A) Elution profiles of tubulin (10 μM) control (●), HsSAS-6 C (10 μM) control (▲) and the mixture of 15 μM tubulin and 10 μM HsSAS-6 C (■) are shown by the plots of absorbance at 280 nm (mAU_{280}) after elution through a Superdex-200 size-exclusion column. The positions of molecular markers (solid arrows), bovine serum albumin (66 kDa), and cytochrome C (12 kDa) are shown. (B, (i) Coomassie blue-stained 12% SDS PAGE gel of eluted protein fractions (as shown in A) collected after loading the mixture of 15 μM tubulin and 10 μM HsSAS-6 C. (B, (ii) 12% SDS PAGE gel of eluted protein fractions collected after loading 10 μM HsSAS-6 C control (as shown in A). (B, (iii) 12% SDS PAGE gel of eluted protein fractions collected after loading 10 μM tubulin control (as shown in A). The gel image represents one of three identical experiments. (C) Isothermal calorimetric titration of HsSAS-6 C with $\alpha\beta$-tubulin dimer. (C) (i) Raw data obtained from 20 injections of 100 μM tubulin (taken in syringe) to 10 μM HsSAS-6 C (taken in cell) in PEM buffer, pH 7.0 at 25 °C. (C, (ii) Nonlinear least-squares fit of the heat changes per mole of added tubulin in the titration shown in (i) as a function of molar ratio of tubulin and HsSAS-6 C by using Origin 7. Data are representative of three identical experiments.

DOI: 10.1021/acs.biochem.5b00978
Biochemistry 2015, 54, 6413−6422

μM) and the small isoforms of Tau ($K_d \approx 0.9$ μM), which are known as microtubule polymerization inducers *in vivo*.[30−33] Although the proteins like CEP135 and CPAP have been implicated to regulate microtubule attachment with the centriolar cartwheel, the triplet microtubules have been found to be associated with the centriolar wall even when these proteins are suppressed.[13] The high binding affinity between HsSAS-6 C and microtubule shown in this study suggests that the C-terminus may play dual roles, promoting microtubule assembly in the centriole and facilitating microtubule attachment with the cartwheel.

As the microtubule polymerizing activity of HsSAS-6 C was suppressed by NaCl (Figure 1D), we next determined how NaCl affects the binding between HsSAS-6 C and microtubule. HsSAS-6 C was added to taxol-polymerized microtubules in the presence of 300 mM NaCl, and the dissociation constant of HsSAS-6 C-microtubule binding was determined by cosedimentation analysis. HsSAS-6 C-microtubule binding was significantly weakened in the presence of NaCl with its K_d increased by ∼3-fold compared with that in the absence of NaCl (Figure 3B i−iii). This weakening of microtubule-HsSAS-6 C binding affinity in the presence of NaCl could presumably be due to shielding of charge−charge interaction between the positively charged amino acids of HsSAS-6 C and the negatively charged microtubules. We therefore checked whether the region (546−638) of HsSAS-6 C, hereafter termed as HsSAS-6 C′ (Figure 3C (i), which consists of a majority (80%) of the positively charged amino acids (10 Lys and 6 Arg) in HsSAS-6 C, can bind to the microtubules. Co-sedimentation analysis with taxol-polymerized microtubules showed that HsSAS-6 C′ associated with the microtubules as equally well as HsSAS-6 C (Figure 3C (ii). We also found that like HsSAS-6 C, HsSAS-6 C′ was equally effective in nucleating and promoting microtubule polymerization *in vitro* (Figure S3A of the Supporting Information). These results suggest that the region 546−638 (HsSAS-6 C′) could play a very critical role in the stabilization of centriolar microtubules.

HsSAS-6 C Binds to Tubulin Dimer *in Vitro*. We next determined the binding of HsSAS-6 C with the $\alpha\beta$-tubulin dimer *in vitro* by size exclusion chromatography and calorimetric titration. A mixture of HsSAS-6 C and tubulin was loaded onto a Superdex 200 size exclusion column, and the eluted protein fractions were analyzed by measuring absorbance of the eluted proteins. The free tubulin dimer and HsSAS-6 C were eluted at 13.4 and 15.4 mL, respectively, whereas the mixture of tubulin and HsSAS-6 C (at 1.5:1 molar ratio) showed an additional peak at 12.8 mL (Figure 4A). SDS−PAGE followed by Coomassie staining of the eluted fractions at 12.8 mL (fraction no. 34) or nearer showed the presence of both HsSAS-6 C and tubulin in these fractions (Figure 4B). These results indicate that HsSAS-6 C associates with the tubulin dimer.

The details of the binding parameters between HsSAS-6 C and $\alpha\beta$-tubulin dimer were then determined by isothermal titration calorimetry (ITC) (Figure 4C). HsSAS-6 C (10 μM) was titrated with a 10-fold molar excess of $\alpha\beta$-tubulin dimer. The heat of dilution profile exhibited the binding reaction between HsSAS-6 C and tubulin as endothermic with a favorable negative enthalpy change (ΔH) of −103.3 ± 5.6 kcal/mol and yielded a dissociation constant (K_d) of 67 ± 5 μM (three experiments). The Gibbs free energy change (ΔG) of the reaction was −5.8 kcal/mol despite a slightly negative entropy change (−327 ± 19 cal/mol/deg), indicating that the binding reaction was predominantly enthalpy driven. No significant binding was observed when HsSAS-6 N was titrated with tubulin (Figure S3B of the Supporting Information).

Previous studies have shown that HsSAS-6 interacts with CEP135, which binds to the centriolar microtubules. Here, we have shown that the C-terminus of HsSAS-6 exerts direct interaction with the microtubules and it exhibits microtubule assembly promoting activity (Figures 1−3). The C-terminus of HsSAS-6 has been shown to be essential for centriole duplication and progression of cells to mitosis *in vivo*.[19] However, the molecular mechanism of the C-terminus in centriole regulation has been poorly understood. The results of the present study are suggestive of an additional mechanism whereby HsSAS-6 could directly interact with the centriolar microtubules through its C-terminus and promote microtubule assembly in the centriole. How could HsSAS-6 simultaneously bind to CEP135 and regulate microtubule assembly in the centriole? A previously proposed model on the attachment of centriole cartwheel with A microtubules has shown that a significant portion of HsSAS-6 toward its C-terminal tail region (537−657) is free from CEP135-binding and is flanked toward the centriolar microtubule wall.[13] Specifically, HsSAS-6 binds CEP135 through its 307−536 region,[13] which contains a significant part of its central coiled-coil domain followed by a small stretch (about 50 residues) of the C-terminus. As both the terminal 470−657 region (HsSAS-6 C) and 546−638 region (HsSAS-6 C′) are equally efficient in microtubule binding and in promoting microtubule assembly (Figures 1 and 3 and Figure S3A of the Supporting Information), it is possible that HsSAS-6 regulates centriolar microtubule assembly predominantly through the 546−638 region, while its central coiled-coil region can still be bound with CEP135. However, the feasibility of this mechanism needs to be tested. As CEP135 also binds to microtubules,[13] a synergistic or antagonistic action between these two proteins on centriolar microtubule stabilization cannot be ruled out.

We have identified in this study a previously unidentified role of the C-terminal tail of human SAS-6 that it nucleates and promotes microtubule assembly through a direct interaction with tubulin and microtubules, functions that may be linked to regulation of centriolar triplet microtubules *in vivo*. Defective centriolar microtubule assembly has been known to cause abnormality in centriole structure and aberrant amplification of centrioles, phenomena that are commonly linked to diseases such as tumors and ciliopathies.[5,34] It will be interesting to explore in the future if SAS-6 C-terminus-mediated microtubule regulation bears any functional link with the pathogenesis of these diseases.[34]

■ ASSOCIATED CONTENT

Supporting Information

The Supporting Information is available free of charge on the ACS Publications website at DOI: 10.1021/acs.biochem.5b00978.

SDS-PAGE analysis of purified proteins, CD spectra of purified proteins, immunofluorescence images of DMSO-polymerized microtubules, turbidity assay with HsSAS-6 C′ and isothermal titration calorimetric analysis of tubulin with HsSAS-6 N (PDF)

DOI: 10.1021/acs.biochem.5b00978
Biochemistry 2015, 54, 6413−6422

AUTHOR INFORMATION

Corresponding Author

*Phone: +(91)-471-2599425; fax: +(91)-471-2597438; e-mail: tmanna@iisertvm.ac.in.

Funding

Financial support from DAE, Govt. of India is thankfully acknowledged.

Notes

The authors declare no competing financial interest.

ACKNOWLEDGMENTS

We thank Dr. P. Gönczy, Swiss Institute for Experimental Cancer research, Lussane, SW for providing human SAS-6 plasmid. We thank Dr. Mani Ramaswamy lab, Centre for Cellular and Molecular Platforms, Bangalore for providing ITC instrument.

ABBREVIATIONS

DMEM, Dulbecco's Modified Eagle's medium; DTT, dithioerythritol; FITC, fluorescein isothiocyanate; GTP, guanosine triphosphate; PIPES, piperazine-*N*,*N*′-bis(2-ethanesulfonic acid); PMSF, phenylmethanesulfonylfluoride; EGTA, ethylene glycol-bis(β-aminoethyl ether)-*N*,*N*,*N*′,*N*′-tetraacetic acid; ITC, isothermal titration calorimetry

REFERENCES

(1) Srsen, V., and Merdes, A. (2006) The centrosome and cell proliferation. *Cell Div. 1*, 26.

(2) Luders, J., and Stearns, T. (2007) Microtubule-organizing centres: a re-evaluation. *Nat. Rev. Mol. Cell Biol. 8*, 161−167.

(3) Nigg, E. A., and Stearns, T. (2011) The centrosome cycle: Centriole biogenesis, duplication and inherent asymmetries. *Nat. Cell Biol. 13*, 1154−1160.

(4) Bettencourt-Dias, M., and Glover, D. M. (2007) Centrosome biogenesis and function: centrosomics brings new understanding. *Nat. Rev. Mol. Cell Biol. 8*, 451−463.

(5) Azimzadeh, J., and Marshall, W. F. (2010) Building the centriole. *Curr. Biol. 20*, R816−825.

(6) Dutcher, S. K. (2003) Elucidation of basal body and centriole functions in Chlamydomonas reinhardtii. *Traffic 4*, 443−451.

(7) O'Toole, E. T., Giddings, T. H., McIntosh, J. R., and Dutcher, S. K. (2003) Three-dimensional organization of basal bodies from wild-type and delta-tubulin deletion strains of Chlamydomonas reinhardtii. *Mol. Biol. Cell 14*, 2999−3012.

(8) Vorobjev, I. A., and Chentsov, Yu. S. (1982) Centrioles in the cell cycle. I. Epithelial cells. *J. Cell Biol. 93*, 938−949.

(9) Kuriyama, R., and Borisy, G. G. (1981) Centriole cycle in Chinese hamster ovary cells as determined by whole-mount electron microscopy. *J. Cell Biol. 91*, 814−821.

(10) Nakazawa, Y., Hiraki, M., Kamiya, R., and Hirono, M. (2007) SAS-6 is a cartwheel protein that establishes the 9-fold symmetry of the centriole. *Curr. Biol. 17*, 2169−2174.

(11) Cottee, M. A., Raff, J. W., Lea, S. M., and Roque, H. (2011) SAS-6 oligomerization: the key to the centriole? *Nat. Chem. Biol. 7*, 650−653.

(12) Guichard, P., Chretien, D., Marco, S., and Tassin, A. M. (2010) Procentriole assembly revealed by cryo-electron tomography. *EMBO J. 29*, 1565−1572.

(13) Lin, Y. C., Chang, C. W., Hsu, W. B., Tang, C. J., Lin, Y. N., Chou, E. J., Wu, C. T., and Tang, T. K. (2013) Human microcephaly protein CEP135 binds to hSAS-6 and CPAP, and is required for centriole assembly. *EMBO J. 32*, 1141−1154.

(14) Hung, L. Y., Chen, H. L., Chang, C. W., Li, B. R., and Tang, T. K. (2004) Identification of a novel microtubule-destabilizing motif in CPAP that binds to tubulin heterodimers and inhibits microtubule assembly. *Mol. Biol. Cell 15*, 2697−2706.

(15) Matsuura, K., Lefebvre, P. A., Kamiya, R., and Hirono, M. (2004) Bld10p, a novel protein essential for basal body assembly in Chlamydomonas: localization to the cartwheel, the first ninefold symmetrical structure appearing during assembly. *J. Cell Biol. 165*, 663−671.

(16) Hiraki, M., Nakazawa, Y., Kamiya, R., and Hirono, M. (2007) Bld10p constitutes the cartwheel-spoke tip and stabilizes the 9-fold symmetry of the centriole. *Curr. Biol. 17*, 1778−1783.

(17) Rodrigues-Martins, A., Bettencourt-Dias, M., Riparbelli, M., Ferreira, C., Ferreira, I., Callaini, G., and Glover, D. M. (2007) DSAS-6 organizes a tube-like centriole precursor, and its absence suggests modularity in centriole assembly. *Curr. Biol. 17*, 1465−1472.

(18) Kitagawa, D., Vakonakis, I., Olieric, N., Hilbert, M., Keller, D., Olieric, V., Bortfeld, M., Erat, M. C., Fluckiger, I., Gonczy, P., and Steinmetz, M. O. (2011) Structural basis of the 9-fold symmetry of centrioles. *Cell 144*, 364−375.

(19) Keller, D., Orpinell, M., Olivier, N., Wachsmuth, M., Mahen, R., Wyss, R., Hachet, V., Ellenberg, J., Manley, S., and Gonczy, P. (2014) Mechanisms of HsSAS-6 assembly promoting centriole formation in human cells. *J. Cell Biol. 204*, 697−712.

(20) Zhang, Y., Xu, T., Chen, Q., Wang, B., and Liu, J. (2011) Expression, purification, and refolding of active human and mouse secreted group IIE phospholipase A(2). *Protein Expression Purif. 80*, 68−73.

(21) Bradford, M. M. (1976) A rapid and sensitive method for the quantitation of microgram quantities of protein utilizing the principle of protein-dye binding. *Anal. Biochem. 72*, 248−254.

(22) Gireesh, K. K., Rashid, A., Chakraborti, S., Panda, D., and Manna, T. (2012) CIL-102 binds to tubulin at colchicine binding site and triggers apoptosis in MCF-7 cells by inducing monopolar and multinucleated cells. *Biochem. Pharmacol. 84*, 633−645.

(23) Singh, P., Thomas, G. E., Gireesh, K. K., and Manna, T. K. (2014) TACC3 protein regulates microtubule nucleation by affecting gamma-tubulin ring complexes. *J. Biol. Chem. 289*, 31719−31735.

(24) Yadav, S., Verma, P. J., and Panda, D. (2014) C-terminal region of MAP7 domain containing protein 3 (MAP7D3) promotes microtubule polymerization by binding at the C-terminal tail of tubulin. *PLoS One 9*, e99539.

(25) Gireesh, K. K., Sreeja, J. S., Chakraborti, S., Singh, P., Thomas, G. E., Gupta, H., and Manna, T. (2014) Microtubule + TIP protein EB1 binds to GTP and undergoes dissociation from dimer to monomer on binding GTP. *Biochemistry 53*, 5551−5557.

(26) van Breugel, M., Hirono, M., Andreeva, A., Yanagisawa, H. A., Yamaguchi, S., Nakazawa, Y., Morgner, N., Petrovich, M., Ebong, I. O., Robinson, C. V., Johnson, C. M., Veprintsev, D., and Zuber, B. (2011) Structures of SAS-6 suggest its organization in centrioles. *Science 331*, 1196−1199.

(27) Larcher, J. C., Boucher, D., Lazereg, S., Gros, F., and Denoulet, P. (1996) Interaction of kinesin motor domains with alpha- and beta-tubulin subunits at a tau-independent binding site. Regulation by polyglutamylation. *J. Biol. Chem. 271*, 22117−22124.

(28) Strnad, P., Leidel, S., Vinogradova, T., Euteneuer, U., Khodjakov, A., and Gonczy, P. (2007) Regulated HsSAS-6 levels ensure formation of a single procentriole per centriole during the centrosome duplication cycle. *Dev. Cell 13*, 203−213.

(29) Puklowski, A., Homsi, Y., Keller, D., May, M., Chauhan, S., Kossatz, U., Grunwald, V., Kubicka, S., Pich, A., Manns, M. P., Hoffmann, I., Gonczy, P., and Malek, N. P. (2011) The SCF-FBXW5 E3-ubiquitin ligase is regulated by PLK4 and targets HsSAS-6 to control centrosome duplication. *Nat. Cell Biol. 13*, 1004−1009.

(30) Coffey, R. L., and Purich, D. L. (1995) Non-cooperative binding of the MAP-2 microtubule-binding region to microtubules. *J. Biol. Chem. 270*, 1035−1040.

(31) Panda, D., Samuel, J. C., Massie, M., Feinstein, S. C., and Wilson, L. (2003) Differential regulation of microtubule dynamics by three- and four-repeat tau: implications for the onset of neurodegenerative disease. *Proc. Natl. Acad. Sci. U. S. A. 100*, 9548−9553.

DOI: 10.1021/acs.biochem.5b00978
Biochemistry 2015, 54, 6413−6422

(32) Makrides, V., Massie, M. R., Feinstein, S. C., and Lew, J. (2004) Evidence for two distinct binding sites for tau on microtubules. *Proc. Natl. Acad. Sci. U. S. A. 101*, 6746−6751.
(33) Friden, B., Wallin, M., Deinum, J., Prasad, V., and Luduena, R. (1987) Effect of estramustine phosphate on the assembly of trypsin-treated microtubules and microtubules reconstituted from purified tubulin with either tau, MAP2, or the tubulin-binding fragment of MAP2. *Arch. Biochem. Biophys. 257*, 123−130.
(34) Nigg, E. A., and Raff, J. W. (2009) Centrioles, centrosomes, and cilia in health and disease. *Cell 139*, 663−678.

DOI: 10.1021/acs.biochem.5b00978
Biochemistry 2015, 54, 6413−6422